Noname manuscript No.
(will be inserted by the editor)

An a-posteriori error estimate for *hp*-adaptive DG methods for elliptic eigenvalue problems on anisotropically refined meshes

Stefano Giani · Edward Hall

Received: date / Accepted: date

Abstract We prove an a-posteriori error estimate for an *hp*-adaptive discontinuous Galerkin method for the numerical solution of elliptic eigenvalue problems with discontinuous coefficients on anisotropically refined rectangular elements. The estimate yields a global upper bound of the errors for both the eigenvalue and the eigenfunction and lower bound of the error for the eigenfunction only. The anisotropy of the underlying meshes is incorporated in the upper bound through an alignment measure. We present a series of numerical experiments to test the flexibility and robustness of this approach within a fully automated *hp*-adaptive refinement algorithm.

1 Introduction

Eigenvalue problems appear naturally in many physical situations, for example, when studying acoustics and vibration analysis, the Schrödinger equation, nuclear reactor criticality and the linear stability analysis of steady solutions to nonlinear differential equations. In this article we consider the following model problem:

$$\begin{cases} -\nabla \cdot (\mathrm{A}\nabla u) = \lambda u & \text{in } \Omega \subset \mathbb{R}^d, \\ u = 0 & \text{on } \Gamma\ , \end{cases} \tag{1.1}$$

S. Giani
School of Mathematical Sciences, University of Nottingham, University Park, Nottingham, NG7 2RD, UK
E-mail: stefano.giani@nottingham.ac.uk

E. Hall
School of Mathematical Sciences, University of Nottingham, University Park, Nottingham, NG7 2RD, UK
E-mail: edward.hall@nottingham.ac.uk

where $d = 2, 3$ and the (generally) matrix-valued function A is real symmetric and uniformly positive definite, i.e.,

$$0 < \underline{a} \leq \xi^t \mathrm{A}(x)\xi \leq \overline{a} \quad \text{for all} \quad \xi \in \mathbb{R}^n \quad \text{with} \quad |\xi| = 1 \quad \text{and all} \quad x \in \Omega\,, \tag{1.2}$$

where Ω is a bounded polyhedral domain with boundary $\Gamma = \partial\Omega$. The standard weak formulation of (1.1) is to find $u \in H_0^1(\Omega)$ such that

$$A(u, v) \equiv \int_\Omega \mathrm{A}\nabla u \cdot \nabla v \, dx = \lambda \int_\Omega u \, v \, dx \equiv \lambda \, b(u, v) \qquad \forall \, v \in H_0^1(\Omega), \tag{1.3}$$

where the space $H_0^1(\Omega)$ is the standard space of functions with gradient in $L^2(\Omega)$ and with zero trace on Γ.

In many situations, for example, when A has discontinuities or in the case of irregularly shaped domains, anisotropy in the eigenfunctions becomes apparent. If we use a finite element type method to solve (1.1) (see [1] for an up to date review) then using anisotropic mesh refinement and polynomial enrichment is likely to resolve these features in a computationally efficient way. In order to drive such an adaptive refinement method, we need robust *a posteriori* error estimates suitable for use on anisotropically refined meshes.

In this article we advocate the use of discontinuous Galerkin (DG) methods for the solution of (1.1), due to the advantages they offer over standard conforming FEMs in the context of *hp*–adaptivity. For example, they provide increased flexibility in mesh design (irregular grids are admissible) and the freedom to choose the elemental polynomial degrees without the need to enforce continuity between elements. Although *a posteriori* error analysis is a mature subject for source problems, for the approximation of eigenvalue problems relatively little work has been done; for the conforming FEM we refer the reader to [27,28,26,13] in the case of residual based error estimates and to [24] for a goal oriented approach; for a DG method, see our recent paper [37], where a robust residual error estimator is presented on isotropically refined grids, and [23,10] where the goal oriented approach is applied, the latter on anisotropic meshes. To the authors' knowledge, the work here represents a first attempt at residual based *a posteriori* error estimation for a DG method applied to an eigenvalue problem on anisotropic grids.

The paper is structured as follows. In the next section we introduce the Symmetric Weighted Interior Penalty (SWIP) DG discretisation of the model problem after first defining some appropriate functions spaces and trace operators. Following this we define some crucial norms and an important identity result. The anisotropic *a posteriori* error estimator is stated in Section 3 and a proof of its reliability given, up to higher order terms. The proof of reliability follows the same general idea as that presented in [37], which in turn followed from work in [14,9,12]. In Section 4 we present three numerical experiments to validate our theoretical results. In all cases exponential rates of convergence are attained under the anisotropic *hp*–adaptation strategy and are seen to be superior to an isotropic *hp*–adaptive strategy.

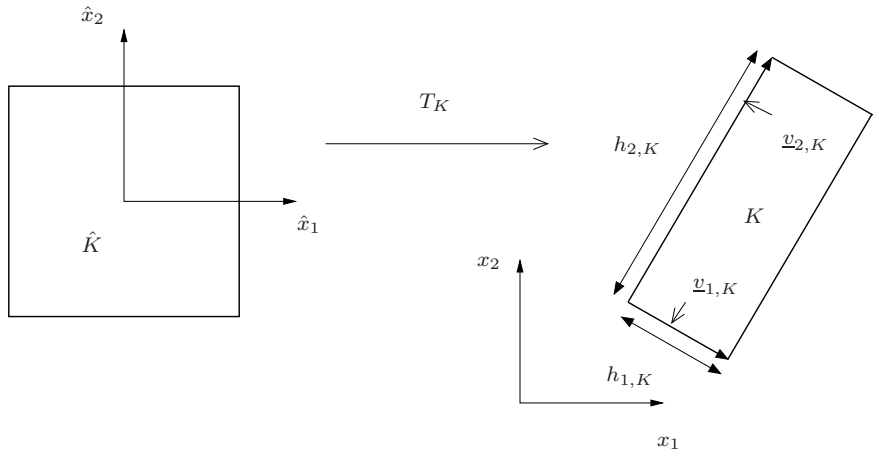

Fig. 1 Affine mapping of the reference element $\hat{K}$ to an (anisotropic) global element K.

2 Discontinuous Galerkin discretization

In this section, we introduce the *hp*-version Symmetric Weighted Interior Penalty (SWIP) DG method for the discretization of (1.1), see [8].

Throughout, we assume that the computational domain Ω can be partitioned into a mesh $\mathcal{T}$ comprising hyper-rectangular elements, where each element $K \in \mathcal{T}$ is the image of the reference hypercube $(-1,1)^d$ under an affine element mapping T_K. For each element K we denote by $h_{i,K}$, $i = 1, \ldots, d$ the measurements of K, we also define for each element:

$$h_{\min,K} := \min_{i=1}^{d}\{h_{i,K}\}, \quad h_{\max,K} := \max_{i=1}^{d}\{h_{i,K}\}.$$

We then define the matrix

$$\mathbf{M}_K = [\underline{v}_{1,K}, \ldots, \underline{v}_{d,K}],$$

where $\{\underline{v}_{i,K}\}_{i=1}^{d}$ are the vectors defining the edges of K of length $\{h_{i,K}\}_{i=1}^{d}$, respectively. See Fig 2 for an example when $d = 2$.

Remark 1 We remark that, for the analysis which follows, the elemental mappings need not be affine, but rather can be composed of an affine mapping and a C^1–diffeomorphism which is sufficiently close to the identity. Please see, for example, [35].

We refer to F as an interior mesh face of $\mathcal{T}$ if $F = \partial K \cap \partial K'$ for two neighbouring elements $K, K' \in \mathcal{T}$ whose intersection has a positive surface measure. The set of all interior mesh faces is denoted by $\mathcal{F}_I(\mathcal{T})$. Analogously, if the intersection of the boundary of an element $K \in \mathcal{T}$ and Γ, i.e. $F = \partial K \cap \Gamma$, is of positive surface measure, we refer to F as a boundary mesh face of $\mathcal{T}$.

The set of all boundary mesh faces of $\mathcal{T}$ is denoted by $\mathcal{F}_B(\mathcal{T})$ and we set $\mathcal{F}(\mathcal{T}) = \mathcal{F}_I(\mathcal{T}) \cup \mathcal{F}_B(\mathcal{T})$. The diameter of a face F is denoted by h_F. We allow for 1-irregularly refined meshes $\mathcal{T}$ defined as follows. Let K be an element of $\mathcal{T}$ and F an elemental face in $\mathcal{F}(K)$. Then F may contain at most one hanging node located in the center of F and at most one hanging node in the middle of each elemental edge of F.

Let us also define for any $F \in \mathcal{F}(\mathcal{T})$ the value $h^{\perp}_{F,K}$ as the diameter of K in the direction perpendicular to F and similarly the value $h_{F,K}$ as the measure of F. For any face $F \in \mathcal{F}(\mathcal{T})$, we further define

$$h^{\perp}_F = \begin{cases} \min\{h^{\perp}_{F,K}, h^{\perp}_{F,K'}\}, & \text{if } F = \partial K \cap \partial K' \in \mathcal{F}_I(\mathcal{T}), \\ h^{\perp}_{F,K}, & \text{if } F = \partial K \cap \Gamma \in \mathcal{F}_B(\mathcal{T}). \end{cases} \tag{2.4}$$

Moreover, for any $F \in \mathcal{F}_I(\mathcal{T})$, we assume that

$$h^{\perp}_{F,K} \sim h^{\perp}_{F,K'}, \quad F = K \cap K' \ .$$

We denote by $h_{\max,i}$, with $i = 1, \ldots, d$, the maximum of the $h_{i,K}$, for all K. Finally we define

$$h_{\min,F} = \begin{cases} \min\{h_{\min,K}, h_{\min,K'}\}, & \text{if } F = \partial K \cap \partial K' \in \mathcal{F}_I(\mathcal{T}), \\ h_{\min,K}, & \text{if } F = \partial K \cap \Gamma \in \mathcal{F}_B(\mathcal{T}). \end{cases} \tag{2.5}$$

We notice that $h^{\perp}_F \sim h^{\perp}_{F,K}$ and, due to the fact that we consider meshes with one hanging node per face, we also have $h_{\min,F} \sim h_{\min,K}$.

In the work that follows we assume an approximation by tensor–product polynomial spaces, hence for an element K it is natural to associate a polynomial degree $p_{i,K}$ with each direction $\underline{v}_{i,K}$, $i = 1, \ldots, d$. We can now make the following definition:

$$p_{\min,K} \ := \ \min_{i=1}^{d}\{p_{i,K}\} \ , \quad p_{\max,K} \ := \ \max_{i=1}^{d}\{p_{i,K}\} \ ,$$

For a face $F \in \mathcal{F}(\mathcal{T})$, we define $p_{F,K} := \max_{j \neq i} p_{j,K}$, and $p^{\perp}_{F,K} := p_{i,K}$ if F is perpendicular to $\underline{v}_{i,K}$, for $i = 1, \ldots, d$. Moreover, we assume that, for all $F \in \mathcal{F}_I(\mathcal{T})$, we have

$$p^{\perp}_{F,K} \sim p^{\perp}_{F,K'} \ , \quad p_{F,K} \sim p_{F,K'} \ ,$$

where K and K' share the same face F. Then, for any edge $F \in \mathcal{F}(\mathcal{T})$, we also introduce the notations:

$$p^{\perp}_F = \begin{cases} \max\{p^{\perp}_{F,K}, p^{\perp}_{F,K'}\}, & \text{if } F = \partial K \cap \partial K' \in \mathcal{F}_I(\mathcal{T}), \\ p^{\perp}_{F,K}, & \text{if } F = \partial K \cap \Gamma \in \mathcal{F}_B(\mathcal{T}), \end{cases} \tag{2.6}$$

$$p_{\max,F} = \begin{cases} \max\{p_{\max,K}, p_{\max,K'}\}, & \text{if } F = \partial K \cap \partial K' \in \mathcal{F}_I(\mathcal{T}), \\ p_{\max,K}, & \text{if } F = \partial K \cap \Gamma \in \mathcal{F}_B(\mathcal{T}). \end{cases} \tag{2.7}$$

We also define $p_{\min,i}$, with $i = 1, \ldots, d$, the minimum of the $p_{i,K}$, for all K. Finally we define for each element K a vector $\mathbf{p}_K := \{p_{1,K}, \ldots, p_{d,K}\}$.

Next, let us define the jumps and averages of piecewise smooth functions across faces of the mesh $\mathcal{T}$. To that end, let the interior face $F \in \mathcal{F}_I(\mathcal{T})$ be shared by two neighbouring elements K^+ and K^-. For a piecewise smooth function v, we denote by v^+ the trace on F taken from inside K, and by v^- the one taken from inside K^-. Let us introduce the non–negative weights w^+ and w^- with the property that $w^+ + w^- = 1$. Then, the (weighted) average and jump of v across the face F are defined as

$$\{\!\{v\}\!\}_w = w^- v^+ + w^+ v^-, \qquad [\![v]\!] = v^+ \, \underline{n}_K^+ + v^- \, \underline{n}_K^-.$$

Here, $\underline{n}_K^+$ and $\underline{n}_K^-$ denote the unit outward normal vectors on the boundary of elements K^+ and K^-, respectively. Similarly, if $\underline{q}$ is a piecewise smooth vector field, its (weighted) average and (normal) jump across F are given by

$$\{\!\{\underline{q}\}\!\}_w = w^+ \underline{q}^+ + w^- \underline{q}^-, \qquad [\![\underline{q}]\!] = \underline{q}^+ \cdot \underline{n}_K^+ + \underline{q}^+ \cdot \underline{n}_K^-.$$

On a boundary face $F \in \mathcal{F}_B(\mathcal{T})$, we accordingly set $\{\!\{\underline{q}\}\!\}_w = \underline{q}$ and $[\![v]\!] = v\underline{n}$, with $\underline{n}$ denoting the unit outward normal vector on Γ. The other trace operators will not be used on boundary faces and are thereby left undefined.

In order to define the *hp*-version finite element space on $\mathcal{T}$, we begin by introducing polynomial spaces on elements. To that end, let $K \in \mathcal{T}$ be an element. We set

$$\mathcal{Q}_{\mathbf{p}_K}(K) = \{\, v \,:\, K \to \mathbb{R} \,:\, v \circ T_K \in \mathcal{Q}_{\mathbf{p}_{\widehat{K}}}(\widehat{K}) \,\}, \tag{2.8}$$

with $\mathcal{Q}_{\mathbf{p}_{\widehat{K}}}(\widehat{K})$ denoting the set of tensor product polynomials on the reference element $\widehat{K}$ of degree less than or equal to $p_{i,\widehat{K}}$ in the x_i-direction, $i = 1, \ldots, d$ on $\widehat{K}$. We then introduce the set of degree vectors $\underline{\mathbf{p}} = \{\, \mathbf{p}_K \,:\, K \in \mathcal{T} \,\}$.

For a partition $\mathcal{T}$ of Ω and polynomial degree vectors $\underline{\mathbf{p}}$ and $\mathcal{T}$, we define the *hp*-version DG finite element space by

$$S_{\underline{\mathbf{p}}}(\mathcal{T}) = \{\, v \in L^2(\Omega) \,:\, v|_K \in \mathcal{Q}_{\mathbf{p}_K}(K),\ K \in \mathcal{T} \,\}. \tag{2.9}$$

The SWIP DG discrete version of the eigenvalue problem (1.3) is: find $(\lambda_{hp}, u_{hp}) \in \mathbb{R} \times S_{\underline{\mathbf{p}}}(\mathcal{T})$ such that

$$A_{hp}(u_{hp}, v_{hp}) = \lambda_{hp} \; b(u_{hp}, v_{hp}) \qquad \forall\, v_{hp} \in S_{\underline{\mathbf{p}}}(\mathcal{T}), \tag{2.10}$$

and with $\|u_{hp}\|_{0,\Omega} = 1$. The bilinear form $A_{hp}(u, v)$ is given by

$$\begin{aligned} A_{hp}(u, v) = & \sum_{K \in \mathcal{T}} \int_K \mathrm{A} \nabla u \cdot \nabla v \, dx - \sum_{F \in \mathcal{F}(\mathcal{T})} \int_F \Big(\{\!\{\mathrm{A} \nabla u\}\!\}_w \cdot [\![v]\!] + \{\!\{\mathrm{A} \nabla v\}\!\}_w \cdot [\![u]\!] \Big) \, ds \\ & + \sum_{F \in \mathcal{F}(\mathcal{T})} \frac{\gamma (p_F^\perp)^2}{h_F^\perp} \int_F [\![u]\!] \cdot [\![v]\!] \, ds, \end{aligned} \tag{2.11}$$

where the gradient operator ∇ is defined elementwise and the parameter $\gamma > 0$ is the interior penalty parameter. We remark that the bilinear form represents an extension of the one presented in [8] to the anisotropic case, with the modifications suggested in [34]; in particular the penalty parameter has been modified to cope with anisotropicity. Finally we must make suitable choices for the weights w^+ and w^- and the penalty parameter γ. First, if $F \in \mathcal{F}_I(\mathcal{T})$, define $\delta_F^{\pm} = \underline{n}_F^{\top} \mathrm{A}^{\pm} \underline{n}_F$, where $\underline{n}_F$ is a unit normal vector to F and similarly, for $F \in \mathcal{F}_B(\mathcal{T})$ let $\delta_F = \underline{n}^{\top} \mathrm{A} \underline{n}$. On an interior face $F \in \mathcal{F}_I(\mathcal{T})$ we then set

$$w^- = \frac{\delta_F^+}{\delta_F^+ + \delta_F^-}, \quad w^+ = \frac{\delta_F^-}{\delta_F^+ + \delta_F^-}$$

and

$$\gamma = \alpha \frac{\delta_F^+ \delta_F^-}{\delta_F^+ + \delta_F^-},$$

here, α is a positive scalar. On a boundary face $F \in \mathcal{F}_B(\mathcal{T})$ we set $\gamma = \alpha \delta_F$. With these selections the method is known to be a stable and consistent method for values of penalty α sufficiently large, see [8].

To be able to carry on the a posteriori analysis, we must perform a non-consistent reformulation of the DG discretization (2.10). To this end, we introduce the following lifting operator already used in [16,2], but with suitable modifications. For any v belonging to $\mathcal{S}(h) := S_{\underline{p}}(\mathcal{T}) + H^2(\mathcal{T}) \cap H^1(\Omega)$, where $H^2(\mathcal{T}) := \{v \in L^2(\Omega) : |v|_K \in H^2(K), \forall K \in \mathcal{T}\}$, we define $\mathcal{L}(v) \in [S_{\underline{\mathbf{p}}}(\mathcal{T})]^2$ by

$$\int_\Omega \mathcal{L}(v) \cdot \mathbf{q}_{hp} \, dx \;=\; \sum_{F \in \mathcal{F}(\mathcal{T})} \int_F [\![v]\!] \cdot \{\!\{ \mathbf{q}_{hp} \}\!\}_w \, ds \;, \quad \forall \mathbf{q}_{hp} \in [S_{\underline{\mathbf{p}}}(\mathcal{T})]^2 \;. \quad (2.12)$$

Now the following extended bilinear form $\tilde{A}_{hp}(u, v)$ can be introduced:

$$\begin{aligned} \tilde{A}_{hp}(u, v) = & \sum_{K \in \mathcal{T}} \int_K \mathrm{A} \nabla u \cdot \nabla v \, dx - \sum_{K \in \mathcal{T}} \int_K \mathcal{L}(u) \cdot \mathrm{A} \nabla v + \mathcal{L}(v) \cdot \mathrm{A} \nabla u \, dx \\ & + \sum_{F \in \mathcal{F}(\mathcal{T})} \frac{\gamma (p_F^{\perp})^2}{h_F^{\perp}} \int_F [\![u]\!] \cdot [\![v]\!] \, ds. \end{aligned} \quad (2.13)$$

Remark 2 It is clear that $\tilde{A}_{hp}(\cdot, \cdot) \equiv A_{hp}(\cdot, \cdot)$ on $S_{\underline{\mathbf{p}}}(\mathcal{T}) \times S_{\underline{\mathbf{p}}}(\mathcal{T})$ and $\tilde{A}_{hp}(\cdot, \cdot) \equiv A(\cdot, \cdot)$ on $H_0^1(\Omega) \times H_0^1(\Omega)$.

We need several norms in the analysis. The standard L^2 norm is denoted by $\| \cdot \|_{0,\Omega}$ and the standard H^1 norm is denoted by $\| \cdot \|_{1,\Omega}$.

Finally, we denote with $\| \cdot \|_{s,\Omega}$ the norm of the Sobolev space $H^s(\Omega)$, with $s \geq 1$ and when we need to restrict a norm to a subpart $\mathcal{B}$ of the domain Ω, we will state this explicitly, for example by $\| \cdot \|_{0,\mathcal{B}}$, $\| \cdot \|_{1,\mathcal{B}}$, etc.

We shall also need the following energy norm which represents a minor modification to that presented in [21]:

Definition 1 (Energy norm) For any $u \in \mathcal{S}(h)$ and for $\gamma > 0$

$$\| u \|^2_{\mathrm{E},\mathcal{T}} = \sum_{K\in\mathcal{T}} \|\mathrm{A}^{1/2}\nabla u\|^2_{0,K} + \sum_{F\in\mathcal{F}(\mathcal{T})} \frac{\gamma(p_F^{\perp})^2}{h_F^{\perp}} \|[\![u]\!]\|^2_{0,F}. \tag{2.14}$$

Mimicking the proofs in [16, Lemma 4.3, Lemma 4.4] we can prove that the bilinear form $\tilde{A}_{hp}(\cdot,\cdot)$ is continuous on $S_{\underline{\mathbf{p}}}(\mathcal{T}) + H^1(\Omega)$, i.e.,

$$|\tilde{A}_{hp}(u,v)| \le C_{\tilde{\mathrm{A}}} \| u \|_{\mathrm{E},\mathcal{T}} \, \| v \|_{\mathrm{E},\mathcal{T}} \ , \tag{2.15}$$

with a constant $C_{\tilde{\mathrm{A}}} > 0$ independent of h and p, and that it is also coercive in $H^1_0(\Omega)$, i.e.,

$$\tilde{A}_{hp}(u,u) = \| u \|^2_{\mathrm{E},\mathcal{T}} \ .$$

The distance of an approximate eigenfunction from the true eigenspace is a crucial quantity in the convergence analysis for eigenvalue problems especially in the case of non-simple eigenvalues.

Definition 2 Given a function $v \in L^2(\Omega)$ and a finite dimensional subspace $\mathcal{P} \subset L^2(\Omega)$, we define:

$$\mathrm{dist}(v,\mathcal{P})_{0,\Omega} \ := \ \min_{w\in\mathcal{P}} \|v - w\|_{0,\Omega} \ . \tag{2.16}$$

Similarly, given a function $v \in S_{\underline{\mathbf{p}}}(\mathcal{T})$ and a finite dimensional subspace $\mathcal{P} \subset H^1_0(\Omega)$, we define:

$$\mathrm{dist}(v,\mathcal{P})_{\mathrm{E},\mathcal{T}} \ := \ \min_{w\in\mathcal{P}} \| v - w \|_{\mathrm{E},\mathcal{T}} \ . \tag{2.17}$$

Now let λ_j be any eigenvalue of problem (1.1), we define $E(\lambda_j)$ to be the span of all corresponding eigenfunctions according to (1.1), moreover, we define $E_1(\lambda_j) = \{u \in E(\lambda_j) : \|u\|_{0,\Omega} = 1\}$.

2.1 Identity results

The focus of this subsection is Lemma 1 which links together the two quantities of interest in our convergence analysis, namely the error in the eigenvalues and the error in the eigenfunctions.

Definition 3 (Residual of a linear problem) Let us define the residual for a linear problem $-\nabla\cdot\mathrm{A}\nabla u = f$, with $f \in L^2(\Omega)$, as

$$\mathcal{R}(u,v) \ := \ \tilde{A}_{hp}(u,v) - b(f,v) \ , \tag{2.18}$$

where u is the solution of the linear problem and $v \in \mathcal{S}(h)$.

Definition 4 (Residual of the eigenvalue problem) We apply Definition 3 to the eigenvalue case allowing $f = \lambda_j u_j$, so for any eigenpair (λ_j, u_j) of problem (1.1):

$$\mathcal{R}(u_j, v) \ := \ \tilde{A}_{hp}(u_j, v) - \lambda_j b(u_j, v) \ , \tag{2.19}$$

where $v \in \mathcal{S}(h)$.

Lemma 1 (Identity result for the extended form) *Let (λ_l, u_l) be a true eigenpair of problem (1.3) with $\|u_l\|_{0,\Omega} = 1$ and let $(\lambda_{j,hp}, u_{j,hp})$ be a computed eigenpair of problem (2.10) with $\|u_{j,hp}\|_{0,\Omega} = 1$. Then we have:*

$$\tilde{A}_{hp}(u_l - u_{j,hp}, u_l - u_{j,hp}) \ = \ \lambda_l \|u_l - u_{j,hp}\|^2_{0,\Omega} \ + \ \lambda_{j,hp} - \lambda_l + 2\mathcal{R}(u_l, u_j - u_{j,hp}).$$

Proof Using the linearity of the bilinear form $\tilde{A}_{hp}(\cdot,\cdot)$ and using (1.3), (2.10); we have

$$\tilde{A}_{hp}(u_l - u_{j,hp}, u_l - u_{j,hp}) \ = \ \lambda_l + \lambda_{j,hp} - 2\tilde{A}_{hp}(u_l, u_{j,hp}) + 2\lambda_l b(u_l, u_{j,hp}) - 2\lambda_l b(u_l, u_{j,hp}) \ . \tag{2.20}$$

Furthermore, by analogous arguments we obtain

$$\|u_l - u_{j,hp}\|^2_{0,\Omega} \ = \ 2 \ - \ 2b(u_l, u_{j,hp}). \tag{2.21}$$

Substituting (2.21) into (2.20) we obtain

$$\tilde{A}_{hp}(u_l - u_{j,hp}, u_l - u_{j,hp}) \ = \ \lambda_l \|u_l - u_{j,hp}\|^2_{0,\Omega} + \lambda_{j,hp} - \lambda_l - 2\tilde{A}_{hp}(u_l, u_{j,hp}) + 2\lambda_l b(u_l, u_{j,hp}) \ .$$

Finally noticing that $\tilde{A}_{hp}(u_l, u_j) = \lambda_l b(u_l, u_j)$ and using (2.19) we obtain the result.

3 A posteriori analysis

As in [39], we shall make use of an auxiliary 1-irregular mesh $\widetilde{\mathcal{T}}$ of affine quadrilaterals. We construct the auxiliary mesh $\widetilde{\mathcal{T}}$ refining the mesh $\mathcal{T}$ such that no-hanging nodes in $\mathcal{T}$ are hanging nodes in $\widetilde{\mathcal{T}}$ as well.

In the sequel, we shall use the symbols $\lesssim$ and $\gtrsim$ to denote bounds that are valid up to positive constants independent of h and p. In particular the hidden constant may depend on $\underline{a}$ and on $\overline{a}$.

We then introduce the following auxiliary DG finite element space on the mesh $\widetilde{\mathcal{T}}$:

$$S_{\underline{\widetilde{\mathbf{p}}}}(\widetilde{\mathcal{T}}) = \{\, v \in L^2(\Omega) \,:\, v|_{\widetilde{K}} \circ T_{\widetilde{K}} \in \mathcal{Q}_{\widetilde{\mathbf{p}_{\widetilde{K}}}}(\widehat{K}),\ \widetilde{K} \in \widetilde{\mathcal{T}} \,\},$$

where the auxiliary polynomial degree vector $\widetilde{\mathbf{p}_{\widetilde{K}}}$ is defined by $p_{i,\widetilde{K}} = p_{i,K}$ for all children $\widetilde{K} \in \widetilde{\mathcal{T}}$ of an element $K \in \mathcal{T}$.

The next theorem, which comes from [39], defines an averaging operator for the auxiliary mesh $\widetilde{\mathcal{T}}$.

Theorem 1 *There exists an averaging operator* $I_{hp} : S_{\underline{\mathbf{p}}}(\mathcal{T}) \to S^c_{\widetilde{\underline{\mathbf{p}}}}(\widetilde{\mathcal{T}})$*, where*

$$S^c_{\widetilde{\underline{\mathbf{p}}}}(\widetilde{\mathcal{T}}) = S_{\widetilde{\underline{\mathbf{p}}}}(\widetilde{\mathcal{T}}) \cap H^1_0(\Omega) \ , \tag{3.22}$$

that satisfies

$$\sum_{\widetilde{K}\in\widetilde{\mathcal{T}}} \|\nabla(v - I_{hp}v)\|^2_{L^2(\widetilde{K})} \lesssim \sum_{F\in\mathcal{F}(\mathcal{T})} p_F^2 h_{\min,F}^{-2} h_F^{\perp} \|[\![v]\!]\|^2_{L^2(F)}, \tag{3.23}$$

$$\sum_{\widetilde{K}\in\widetilde{\mathcal{T}}} \|v - I_{hp}v\|^2_{L^2(\widetilde{K})} \lesssim \sum_{F\in\mathcal{F}(\mathcal{T})} (p_F^{\perp})^{-2} h_F^{\perp} \|[\![v]\!]\|^2_{L^2(F)}. \tag{3.24}$$

Let $(\lambda_{j,hp}, u_{j,hp})$ eigenpair of (2.10). For each element $K \in \mathcal{T}$, we introduce the following local error indicator $\eta_{j,K}$ which is given by the sum of the three terms:

$$\eta^2_{j,K} = \eta^2_{j,R_K} + \eta^2_{j,F_K} + \eta^2_{j,J_K} \ , \tag{3.25}$$

where the first term η_{j,R_K} is the residual in the interior of the element K:

$$\eta^2_{j,R_K} = p^{-2}_{\min,K} h^2_{\min,K} \|\lambda_{j,hp} u_{j,hp} + \nabla\cdot \mathrm{A}\nabla u_{j,hp}\|^2_{0,K} \ ,$$

the second term η_{j,F_K} is the residual on the faces of K in the interior of the domain Ω:

$$\eta^2_{j,F_K} = \frac{1}{2} \sum_{F\in\mathcal{F}_I(K)} \int_F \frac{h^2_{\min,K} p^{\perp}_{F,K}}{p^2_{\min,K} h^{\perp}_{F,K}} |[\![\mathrm{A}\nabla u_{j,hp}]\!]|^2_{0,F}\, ds \ ,$$

and finally the residual η_{j,J_K} measures the jumps on the faces of K of the approximate solution $u_{j,hp}$:

$$\begin{aligned}\eta^2_{j,J_K} = \frac{1}{2} &\sum_{F\in\mathcal{F}_I(K)} \int_F \Big(\frac{\gamma^2 (p^{\perp}_{F,K})^5 h^2_{\min,K}}{p^2_{\min,K} (h^{\perp}_{F,K})^3} + \frac{\gamma^2 (p^{\perp}_F)^2}{h^{\perp}_F} \Big) |[\![u_{j,hp}]\!]|^2_{0,F}\, ds \\ &+ \sum_{F\in\mathcal{F}_B(K)} \int_F \Big(\frac{\gamma^2 (p^{\perp}_{F,K})^5 h^2_{\min,K}}{p^2_{\min,K} (h^{\perp}_{F,K})^3} + \frac{\gamma^2 (p^{\perp}_F)^2}{h^{\perp}_F} \Big) |[\![u_{j,hp}]\!]|^2_{0,F}\, ds.\end{aligned}$$

Summing (3.25) on all elements we obtain the global error estimator η_j:

$$\eta^2_j = \sum_{K\in\mathcal{T}} \eta^2_{j,K}. \tag{3.26}$$

Definition 5 (Alignment measure) For $v \in H^1(\Omega)$ we define the alignment measure

$$\mathcal{M}(v,\mathcal{T}) = \frac{\big(\sum_{K\in\mathcal{T}} h^{-2}_{\min,K} \|\mathbf{M}_K \nabla v\|^2_{0,K}\big)^{1/2}}{\|\nabla v\|_{0,\Omega}}.$$

In order to prove the reliability, we decompose a computed eigenfunction $u_{j,hp}$ into a conforming part and a remainder:

$$u_{j,hp} = u^c_{j,hp} + u^r_{j,hp},$$

where $u^c_{j,hp} = I_{hp} u_{j,hp} \in S^c_{\underline{\mathbf{p}}}(\widetilde{\mathcal{T}}) \subset H^1_0(\Omega)$ is defined using the averaging operator I_{hp} in Theorem 1 and the remainder $u^r_{j,hp}$ is given by $u^r_{j,hp} = u_{j,hp} - u^c_{j,hp} \in S_{\underline{\mathbf{p}}}(\widetilde{\mathcal{T}})$. It is straightforward to show that $\| u_j - u_{j,hp} \|_{\mathrm{E},\mathcal{T}} \leq \| u_j - u_{j,hp} \|_{\mathrm{E},\widetilde{\mathcal{T}}}$, therefore, since $u_j - u^c_{j,hp} \in H^1_0(\Omega)$,

$$\begin{aligned} \| u_j - u_{j,hp} \|_{\mathrm{E},\mathcal{T}} \leq \| u_j - u_{j,hp} \|_{\mathrm{E},\widetilde{\mathcal{T}}} &\leq \|u_j - u^c_{j,hp}\|_{\mathrm{E},\widetilde{\mathcal{T}}} + \|u^r_{j,hp}\|_{\mathrm{E},\widetilde{\mathcal{T}}} \\ &= \|u_j - u^c_{j,hp}\|_{\mathrm{E},\mathcal{T}} + \|u^r_{j,hp}\|_{\mathrm{E},\widetilde{\mathcal{T}}} \end{aligned} \tag{3.27}$$

Then to prove reliability for eigenfunctions it is just necessary to bound both terms in the right hand side of (3.27) using η_j. The proof that

$$\|u^r_{hp}\|_{\mathrm{E},\widetilde{\mathcal{T}}} \lesssim \eta_j, \tag{3.28}$$

is equivalent to [39, Lemma 5.4.6] and we omit it for brevity.

On the other hand, to bound $\| u_j - u^c_{j,hp} \|_{\mathrm{E},\mathcal{T}}$ in (3.27), we split $A_{hp}(\cdot,\cdot) = D_{hp}(\cdot,\cdot) + K_{hp}(\cdot,\cdot)$ where

$$D_{hp}(u,v) = \sum_{K\in\mathcal{T}} \int_K \mathrm{A}\nabla u \cdot \nabla v \, dx + \sum_{F\in\mathcal{F}(\mathcal{T})} \frac{\gamma(p^\perp_F)^2}{h^\perp_F} \int_F [\![u]\!] \cdot [\![v]\!] \, ds,$$

$$K_{hp}(u,v) = -\sum_{F\in\mathcal{F}(\mathcal{T})} \int_F \{\!\{\mathrm{A}\nabla u\}\!\}_w \cdot [\![v]\!] \, ds - \sum_{F\in\mathcal{F}(\mathcal{T})} \int_F \{\!\{\mathrm{A}\nabla v\}\!\}_w \cdot [\![u]\!] \, ds.$$

The form $D_{hp}(u,v)$ is well-defined for $u, v \in S_{\underline{p}}(\mathcal{T}) + H^1(\Omega)$, whereas $K_{hp}(u,v)$ is only well-defined for discrete functions $u, v \in S_{\underline{p}}(\mathcal{T})$. Furthermore, we have

$$A(u,v) = D_{hp}(u,v) \qquad \forall\, u, v \in H^1_0(\Omega), \tag{3.29}$$

as well as

$$A_{hp}(u,v) = D_{hp}(u,v) + K_{hp}(u,v) \qquad \forall\, u, v \in S_{\underline{p}}(\mathcal{T}). \tag{3.30}$$

We also recall the standard *hp*-approximation results from [39, Lemma 5.4.7]: For any $v \in H^1_0(\Omega)$, there exists a function $v_{hp} \in S_{\underline{p}}(\mathcal{T})$ such that

$$\begin{aligned} p^2_{\min,K} \|v - v_{hp}\|^2_{0,K} &\lesssim \|\mathbf{M}_K \nabla v\|^2_{0,K}, \\ \|\mathbf{M}_K \nabla (v - v_{hp})\|^2_{0,K} &\lesssim \|\mathbf{M}_K \nabla v\|^2_{0,K}, \\ \sum_{F\in\mathcal{F}(K)} \frac{h^\perp_{F,K} p^2_{\min,K}}{p^\perp_{F,K}} \|v - v_{hp}\|^2_{0,F} &\lesssim \|\mathbf{M}_K \nabla v\|^2_{0,K}, \end{aligned} \tag{3.31}$$

for any element $K \in \mathcal{T}$.

Lemma 2 *For any $v \in H_0^1(\Omega)$, we have*

$$\lambda_j b(u_j, v-v_{hp}) - D_{hp}(u_{j,hp}, v-v_{hp}) + K_{hp}(u_{j,hp}, v_{hp}) \lesssim \mathcal{M}(v,\mathcal{T})\Big(\eta_j + \frac{h_{\min}}{p_{\min}}\|\lambda_j u_j - \lambda_{j,hp}u_{j,hp}\|_0\Big)\| v \|_{\mathrm{E},\mathcal{T}}.$$

Here, $v_{hp} \in S_{\underline{p}}(\mathcal{T})$ is the hp-approximation of v satisfying (3.31).

Proof For brevity, let us set

$$T = \int_\Omega \lambda_j u_j (v - v_{hp})\, dx - D_{hp}(u_{j,hp}, v - v_{hp}) + K_{hp}(u_{j,hp}, v_{hp}).$$

Integrating the volume terms by parts we obtain

$$\begin{aligned} T &= \sum_{K\in\mathcal{T}} \int_K (\lambda_j u_j + \nabla\cdot \mathrm{A}\nabla u_{j,hp})(v - v_{hp})\, dx - \sum_{F\in\mathcal{F}(\mathcal{T})} \frac{\gamma (p_F^\perp)^2}{h_F^\perp} \int_F [\![u_{j,hp}]\!] \cdot [\![v - v_{hp}]\!]\, ds \\ &\quad - \sum_{F\in\mathcal{F}_I(\mathcal{T})} \int_F [\![\mathrm{A}\nabla u_{j,hp}]\!] \{\!\{ v - v_{hp} \}\!\}_w\, ds - \sum_{F\in\mathcal{F}(\mathcal{T})} \int_F \{\!\{ \mathrm{A}\nabla v_{hp} \}\!\}_w \cdot [\![u_{j,hp}]\!]\, ds \\ &\equiv T_1 - T_2 - T_3 - T_4. \end{aligned}$$

Using the Cauchy-Schwarz inequality and the approximation properties (3.31) we have that

$$\begin{aligned} T_1 &= \sum_{K\in\mathcal{T}} \int_K (\lambda_{j,hp} u_{j,hp} + \nabla\cdot \mathrm{A}\nabla u_{j,hp})(v - v_{hp})\, dx + \sum_{K\in\mathcal{T}} \int_K (\lambda_j u_j - \lambda_{j,hp}u_{j,hp})(v - v_{hp})\, dx \\ &\lesssim \mathcal{M}(v,\mathcal{T})\Big(\sum_{K\in\mathcal{T}} \eta_{j,R_K}^2\Big)^{\frac{1}{2}} \| v \|_{\mathrm{E},\mathcal{T}} + \mathcal{M}(v,\mathcal{T}) \frac{h_{\min}}{p_{\min}} \|\lambda_j u_j - \lambda_{j,hp}u_{j,hp}\|_0 \| v \|_{\mathrm{E},\mathcal{T}}. \end{aligned}$$

For term T_2, we again exploit the Cauchy-Schwarz inequality to conclude that

$$T_2 \le \Big(\sum_{K\in\mathcal{T}} \sum_{F\in\partial K} \gamma^2 \frac{h_{\min,K}^2 (p_{F,K}^\perp)^5}{p_{\min,K}^2 (h_{F,K}^\perp)^3} \|[\![u_{j,hp}]\!]\|_{0,F}^2\Big)^{\frac{1}{2}} \Big(\sum_{K\in\mathcal{T}} \sum_{F\in\partial K} \frac{p_{\min,K}^2 h_{F,K}^\perp}{h_{\min,K}^2 p_{F,K}^\perp} \|v - v_{hp}\|_{0,F}^2\Big)^{\frac{1}{2}}.$$

Thus, from (3.31), we obtain the bound

$$T_2 \lesssim \mathcal{M}(v,\mathcal{T})\Big(\sum_{K\in\mathcal{T}} \eta_{j,J_K}^2\Big)^{\frac{1}{2}} \| v \|_{\mathrm{E},\mathcal{T}}.$$

Similarly, using the fact that $w^+, w^- \le 1$, term T_3 can be bounded as follows

$$\begin{aligned} T_3 &\le \Big(\sum_{K\in\mathcal{T}} \sum_{F\in\partial K/\partial\Omega} \frac{h_{\min,K}^2 p_{F,K}^\perp}{p_{\min,K}^2 h_{F,K}^\perp} \|[\![\mathrm{A}\nabla u_{j,hp}]\!]\|_{0,F}^2\Big)^{\frac{1}{2}} \Big(\sum_{K\in\mathcal{T}} \sum_{F\in\partial K/\partial\Omega} \frac{p_{\min,K}^2 h_{F,K}^\perp}{h_{\min,K}^2 p_{F,K}^\perp} \|v - v_{hp}\|_{0,F}^2\Big)^{\frac{1}{2}} \\ &\lesssim \mathcal{M}(v,\mathcal{T})\Big(\sum_{K\in\mathcal{T}} \eta_{j,F_K}^2\Big)^{\frac{1}{2}} \| v \|_{\mathrm{E},\mathcal{T}}. \end{aligned}$$

In a similar way we use the Cauchy-Schwarz inequality for term T_4:

$$T_4 \lesssim \gamma^{-1}\Big(\sum_{K\in\mathcal{T}}\sum_{F\in\partial K}\gamma^2\frac{(p_F^{\perp})^2}{h_F^{\perp}}\|[\![u_{j,hp}]\!]\|_{0,F}^2\Big)^{\frac{1}{2}}\Big(\sum_{K\in\mathcal{T}}\sum_{F\in\partial K}\frac{h_F^{\perp}}{(p_F^{\perp})^2}\|\mathrm{A}\nabla v_{hp}\|_{0,\partial K}^2\Big)^{\frac{1}{2}}.$$

From the standard *hp*-version inverse trace inequality, see [40, Lemma 3.1], we conclude that

$$T_4 \lesssim \gamma^{-1}\Big(\sum_{K\in\mathcal{T}}\eta_{j,J_K}^2\Big)^{\frac{1}{2}}\Big(\sum_{K\in\mathcal{T}}\|\mathrm{A}\nabla v_{hp}\|_{0,K}^2\Big)^{\frac{1}{2}},$$

furthermore, using the approximation properties in (3.31),

$$\sum_{K\in\mathcal{T}}\|\mathrm{A}\nabla v_{hp}\|_{0,K}^2 \lesssim \sum_{K\in\mathcal{T}}\|\mathrm{A}\nabla(v-v_{hp})\|_{0,K}^2 + \sum_{K\in\mathcal{T}}\|\mathrm{A}\nabla v\|_{0,K}^2 \lesssim \|\,v\,\|_{\mathrm{E},\mathcal{T}}^2.$$

Hence

$$T_4 \lesssim \gamma^{-1}\Big(\sum_{K\in\mathcal{T}}\eta_{j,J_K}^2\Big)^{\frac{1}{2}}\|\,v\,\|_{\mathrm{E},\mathcal{T}}.$$

The bounds for T_1, T_2, T_3, and T_4 imply the assertion.

Lemma 3 *Let $(\lambda_{j,hp},u_{j,hp})$ be a computed eigenpair of (2.10) and let (λ_j,u_j) be an eigenpair of* (1.3)*. Then we have for $u_{j,hp}^c = I_{hp}\,u_{j,hp}$ that:*

$$\|\,u_j-u_{j,hp}^c\,\|_{\mathrm{E},\mathcal{T}} \lesssim \mathbf{M}(v,\mathcal{T})\Big(\eta_j+\Big(1+\frac{h_{\min}}{p_{\min}}\Big)\|\lambda_j u_j-\lambda_{j,hp}u_{j,hp}\|_0\Big),$$

where $v=u_j-u_{j,hp}^c\in H_0^1(\Omega)$

Proof Since $u_j-u_{j,hp}^c\in H_0^1(\Omega)$, we have that

$$\|\,u_j-u_{j,hp}^c\,\|_{\mathrm{E},\mathcal{T}}^2 = A_{hp}(u_j-u_{j,hp}^c,v) = A(u_j-u_{j,hp}^c,v). \tag{3.32}$$

To bound the right-hand side of (3.32), we note that, by (3.29),

$$A(u_j-u_{j,hp}^c,v) = \int_\Omega \lambda_j u_j v\,dx - A(u_{j,hp}^c,v) = \int_\Omega \lambda_j u_j v\,dx - D_{hp}(u_{j,hp}^c,v).$$

It is straightforward to see that $D_{hp}(u_{j,hp}^c,v) = D_{hp}(u_{j,hp},v)+R$, with

$$R = -\sum_{\widetilde{K}\in\widetilde{\mathcal{T}}}\int_{\widetilde{K}}\mathrm{A}\nabla u_{j,hp}^r\cdot\nabla v\,dx\ .$$

Furthermore, from (2.10) and (3.30), we have

$$\int_\Omega \lambda_{j,hp}u_{j,hp}v_{hp}\,dx = D_{hp}(u_{j,hp},v_{hp}) + K_{hp}(u_{j,hp},v_{hp}),$$

where $v_{hp} \in S_{\underline{p}}(\mathcal{T})$ is the *hp*-approximation of v. Combining these results, we thus arrive at

$$A(u_j - u^c_{j,hp}, v) = \int_\Omega (\lambda_j u_j - \lambda_{j,hp} u_{j,hp}) v_{hp}\, dx + \int_\Omega \lambda_j u_j (v - v_{hp})\, dx$$
$$- D_{hp}(u_{j,hp}, v - v_{hp}) + K_{hp}(u_{j,hp}, v_{hp}) - R\ . \tag{3.33}$$

Using Poincare's inequality and (3.31) we have

$$\|v_{hp}\|_{0,\Omega} \lesssim \mathbf{M}(v,\mathcal{T}) \frac{h_{\min}}{p_{\min}} \|\nabla v\|_{0,\Omega} + \|v\|_{0,\Omega} \leq \Big(\mathbf{M}(v,\mathcal{T}) \frac{h_{\min}}{p_{\min}} + C_p\Big) \|\nabla v\|_{0,\Omega},$$

then from (3.33) we obtain:

$$A(u_j - u^c_{j,hp}, v) \leq \Big(\mathbf{M}(v,\mathcal{T}) \frac{h_{\min}}{p_{\min}} + C_p\Big) \|\lambda_j u_j - \lambda_{j,hp} u_{j,hp}\|_{0,\Omega} \| v \|_{\mathrm{E},\mathcal{T}}$$
$$+ \int_\Omega \lambda_j u_j (v - v_{hp})\, dx$$
$$- D_{hp}(u_{j,hp}, v - v_{hp}) + K_{hp}(u_{j,hp}, v_{hp}) - R.$$

The estimate in Lemma 2 now yields

$$A(u_j - u^c_{j,hp}, v) \lesssim \mathbf{M}(v,\mathcal{T}) \Big(\eta_j + \Big(C_p + \frac{h_{\min}}{p_{\min}}\Big) \|\lambda_j u_j - \lambda_{j,hp} u_{j,hp}\|_0\Big) \| v \|_{\mathrm{E},\mathcal{T}} + |R|. \tag{3.34}$$

It remains to bound $|R|$; from the Cauchy-Schwarz inequality and (3.28), we readily obtain

$$|R| \lesssim \| u^r_{j,hp} \|_{\mathrm{E},\widetilde{\mathcal{T}}} \| v \|_{\mathrm{E},\mathcal{T}} \lesssim \eta_j \| v \|_{\mathrm{E},\mathcal{T}}. \tag{3.35}$$

The desired result now follows from (3.34) and (3.35).

The proof of Theorem 2 readily follows from (3.27), (3.28) and Lemma 3.

Theorem 2 (Reliability for eigenfunctions) *Let $(\lambda_{j,hp}, u_{j,hp})$ be a computed eigenpair of (2.10) converging to the true eigenvalue λ_j of multiplicity $E \geq 1$. Then we have that:*

$$\mathrm{dist}(u_{j,hp}, E_1(\lambda_j))_{\mathrm{E},\mathcal{T}} \lesssim \mathbf{M}(v,\mathcal{T}) \Big(\eta_j + \Big(1 + \frac{h_{\min}}{p_{\min}}\Big)\Big) \|\lambda_j u_j - \lambda_{j,hp} u_{j,hp}\|_0\ ,$$

where u_j is the minimizer of (2.16)*, with $\mathcal{P} = E_1(\lambda_j)$ and $v = u_j - u^c_{j,hp}$.*

Proof From (3.27), (3.28) and Lemma 3 we have that:

$$\mathrm{dist}(u_{j,hp}, E_1(\lambda_j))_{\mathrm{E},\mathcal{T}} \leq \|u_j - u^c_{j,hp}\|_{\mathrm{E},\mathcal{T}} + \|u^r_{j,hp}\|_{\mathrm{E},\widetilde{\mathcal{T}}}$$
$$\lesssim \mathbf{M}(v,\mathcal{T}) \Big(\eta_j + \Big(1 + \frac{h_{\min}}{p_{\min}}\Big)\Big) \|\lambda_j u_j - \lambda_{j,hp} u_{j,hp}\|_0\ .$$

Theorem 3 (Reliability for eigenvalues) *Let $(\lambda_{j,hp}, u_{j,hp})$ be a computed eigenpair of (2.10) and converging to λ_j of multiplicity $E \geq 1$. Then we have that:*

$$|\lambda_j - \lambda_{hp}| \lesssim \mathbf{M}(v,\mathcal{T})^2(\eta_j^2 + G) \ , \tag{3.36}$$

where

$$G = \Big(1+\frac{h_{\min}}{p_{\min}}\Big)^2 \|\lambda_j u_j - \lambda_{j,hp}u_{j,hp}\|_0^2 + 2\eta_j\Big(1+\frac{h_{\min}}{p_{\min}}\Big)\|\lambda_j u_j - \lambda_{j,hp}u_{j,hp}\|_0 + 2|\mathcal{R}(\hat{u}_j, \hat{u}_j - u_{j,hp})|,$$

where u_j is the minimizer of (2.16) and $\hat{u}_j$ is the minimizer of (2.17), with $\mathcal{P} = E_1(\lambda_j)$ in both cases and $v = u_j - u^c_{j,hp}$.

Proof Applying (2.15) to Lemma 1 and also noticing that $\lambda_j\|\hat{u}_j - u_{j,hp}\|^2_{0,\Omega} > 0$ we have

$$|\lambda_j - \lambda_{j,hp}| \lesssim \mathrm{dist}(u_{j,hp}, E_1(\lambda_j))^2_{\mathrm{E},\mathcal{T}} + 2|\mathcal{R}(\hat{u}_j, \hat{u}_j - u_{j,hp})| \ .$$

Applying Theorem 2

$$|\lambda_j - \lambda_{j,hp}| \lesssim \mathbf{M}(v,\mathcal{T})^2\Big(\eta_j + \Big(1+\frac{h_{\min}}{p_{\min}}\Big)\|\lambda_j u_j - \lambda_{j,hp}u_{j,hp}\|_0\Big)^2 + 2|\mathcal{R}(\hat{u}_j, \hat{u}_j - u_{j,hp})|.$$

Remark 3 (Efficiency) It is straightforward to prove efficiency of the error indicator (3.26) using the same techniques as in [37]; we omit the details for brevity. Unfortunately, as with many other works, for example [9,14,15], this efficiency result is robust only in terms of h. However, our numerical experiments indicate the error estimate to be robust in both h and p, even though theoretical results are not available.

4 Numerical Experiments

In this section we present three numerical examples to highlight the performance of the *a posteriori* error estimates when coupled with an anisotropic adaptive *hp*-strategy. In all three of the examples we select $d = 2$ and choose initial grids with only axiparallel elements; in our experience for two-dimensional problems a combination of anisotropic h–refinement with isotropic p-enrichment is often sufficient to obtain highly accurate solutions with minimal computational effort. In all the examples we use $|\eta_{j,K}|$ to determine which elements to refine based on a fixed fraction strategy. The decision to perform h–refinement or p–enrichment is taken by approximating the regularity using the technique described in [31]. If an element has been selected for h–refinement, then we can perform one of two anisotropic refinements, which cut the element in two by bisecting opposite faces, or an isotropic refinement. To make the decision on which we use the method advocated in [38]. Suppose element K has been selected, let F^1_K and F^2_K be the two sets containing the faces parallel to either $\underline{v}_{1,K}$ or $\underline{v}_{2,K}$ and define

$$\eta^2_{F^i_K} = \eta^2_{j,F_K}|_{F^i_K} + \eta^2_{j,J_K}|_{F^i_K} \quad i = 1, 2.$$

The choice between isotropic or anisotropic h–refinement is made by comparing $\eta^2_{F^1_K}$ and $\eta^2_{F^2_K}$. If $\eta^2_{F^1_K} > 10\eta^2_{F^2_K}$ then the element is refined anisotropically in the direction of $\underline{v}_{1,K}$; if on the other hand $\eta^2_{F^2_K} > 10\eta^2_{F^1_K}$ then the element is refined anisotropically in the direction of $\underline{v}_{2,K}$, if neither of these conditions is satisfied then isotropic refinement is carried out. We remark that the refinement parameter is chosen to be 10 based purely on experience. In all of our examples we choose the stabilisation parameter $\alpha = 10$ again based on experience, but with no relation to the refinement parameter.

4.1 Example 1

In our first example we select $\Omega = (0, 0.1) \times (0, 1)$ and let $\mathrm{A} = I$, in which case the eigenvectors have an anisotropic nature influenced by the shape of the domain. We select an initial grid comprising 10 isotropic elements with an initial polynomial degree of 2. We compare an isotropic *hp*–strategy with the anisotropic h–isotropic p–strategy detailed above for the first eigenpair, $(101\pi^2, \sin(10\pi x)\sin(\pi y))$.

A plot showing the convergence of our adaptive anisotropic *hp*–strategy compared with a more standard isotropic *hp*–strategy is shown in Figure 2. We note, on the basis of the a priori analysis in [32, Section 3.4.6, p. 118], we plot the error against the square root of the degrees of freedom ($\mathrm{DOF}^{1/2}$). We notice immediately that the anisotropic strategy is performing extremely well; indeed, on the final grid the anisotropic strategy has achieved an error over 4 orders of magnitude smaller than the isotropic strategy for the same number of degrees of freedom. Figure 3(a) shows a plot of the anisotropically refined mesh together with the polynomial degree distribution after 12 refinement steps. As we would wish, the mesh has been refined in accordance with the anisotropy present in the eigenfunction, which is shown in Figure 5(b). Finally, in Table 1, we show the true error $|\lambda_1 - \lambda_{1,hp}|$, the error bound η_1^2 and the Effectivity $:= \eta_1^2/|\lambda_1 - \lambda_{1,hp}|$. We see that, after mesh number 3 and as the mesh is refined, the effectivity remains bounded between 9 and 30 and is oscillatory, but with small variations. This indicates that the anisotropic error bound is robust in the sense that the hidden constant in (3.36) is independent of both h and p and the extra terms in (3.36) are indeed of higher order.

4.2 Example 2

Our second example is problem (1.1) with $\mathrm{A} = I$ on the H-shaped domain $\Omega = [0, 1]^2/([1/3, 2/3] \times [0, 1/3] \cup [1/3, 2/3] \times [2/3, 1])$. The initial mesh is a conforming structured mesh of 7 elements and the initial order of polynomials is 2. In this example the eigenvalue and eigenfunctions are unknown analytically, but computations on extremely fine meshes reveal that the first eigenvalue is 69.597800 to the accuracy of the computations. As before, Figure 4 shows a comparison of the error committed in approximating the first

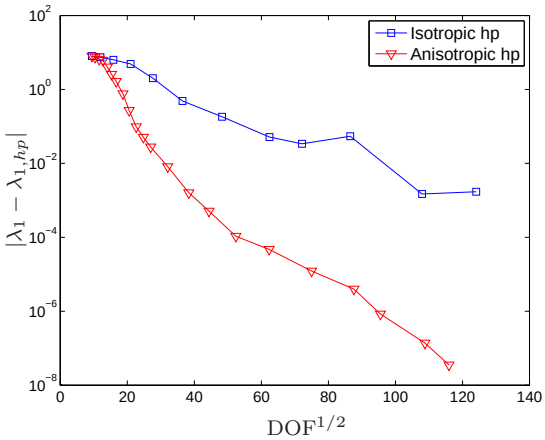

Fig. 2 Example 1: Comparison of isotropic *hp*– and anisotropic *hp*–strategy.

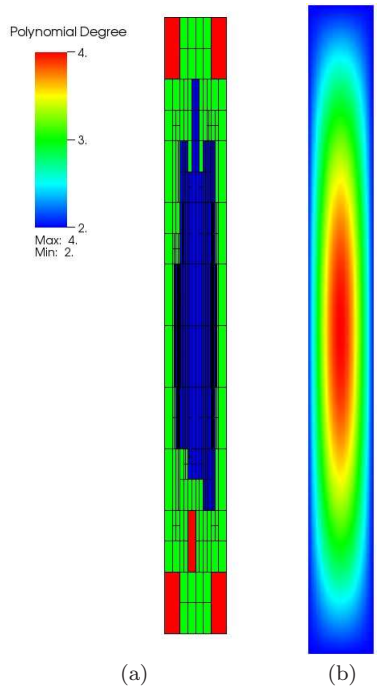

Fig. 3 Example 1: (a) Mesh after 12 anisotropic adaptive refinement steps and (b) first eigenfunction.

DOF	$\lvert\lambda_1 - \lambda_{1,hp}\rvert$	η_1^2	Effectivity
90	8.0403	673.818	83.81
108	7.4433	467.165	62.77
135	6.5666	247.339	37.67
162	6.1466	154.083	25.07
198	4.0506	99.582	24.58
234	2.5646	63.381	24.71
279	1.6484	37.192	22.56
351	7.6326E-01	16.907	22.15
423	2.7082E-01	5.909	21.82
514	9.8094E-02	1.853	18.89
615	5.0994E-02	1.122	22.00
729	2.7859E-02	5.171E-01	18.56
1029	8.1173E-03	1.492E-01	18.38
1472	1.6110E-03	2.943E-02	18.26
1971	5.1050E-04	8.839E-03	17.31
2746	1.0669E-04	1.680E-03	15.75
3886	4.7267E-05	5.390E-04	11.40
5621	1.2214E-05	1.616E-04	13.23
7678	3.9858E-06	4.725E-05	11.86
9123	8.3852E-07	7.816E-05	9.32
11840	1.3767E-07	2.516E-06	18.27
13451	3.5347E-08	5.637E-07	15.95

Table 1 Example 1: Anisotropic *hp*–strategy effectivities.

eigenvalue when the isotropic and anisotropic adaptive strategies are applied. On basis of the a priori analysis in [41], we assume an error model of the form

$$\lambda_{j,h} = \lambda_j + Ce^{-2\gamma\sqrt[3]{\mathrm{DOF}}},$$

for problems with discontinuous coefficients or reentrant corners and thus plot the error against $\mathrm{DOF}^{1/3}$. In this case we do not witness such a dramatic improvement in the convergence as we saw for Example 1, nonetheless, the anisotropic strategy is consistently superior to the isotropic strategy and on the final grid the error is approaching one order of magnitude smaller for the same number of degrees of freedom. If we consider Figure 5(b) we notice that, although there are areas in the domain where the eigenfunction has anisotropy, the eigenfunction has singularities around the reentrant corners. We see in Figure 5(a) that a combination of anisotropic and isotropic refinement has been carried out, with isotropic refinement focused on the reentrant corners. Again, in Table 4.2 we show the effectivities as the mesh is refined. Similarly to Example 1, the effectivity is bounded between 9 and 30 after the 2nd mesh, although the effectivity seems to be growing after the 9th mesh. Ideally we would wish to have data from another one or two meshes to confirm the effectivity does remain bounded, but we were hampered by the lack of a more accurate reference eigenvalue. Nonetheless, the results do indicate robustness of the error estimate.

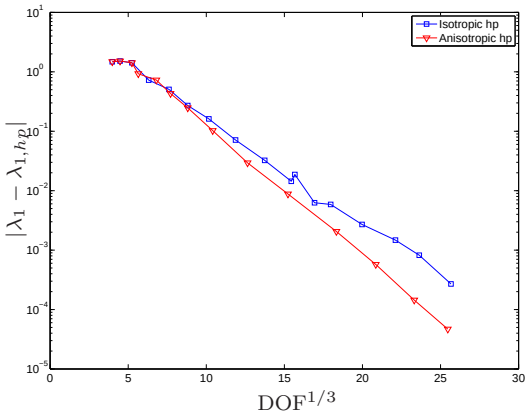

Fig. 4 Example 2: Comparison of isotropic *hp*– and anisotropic *hp*–strategy.

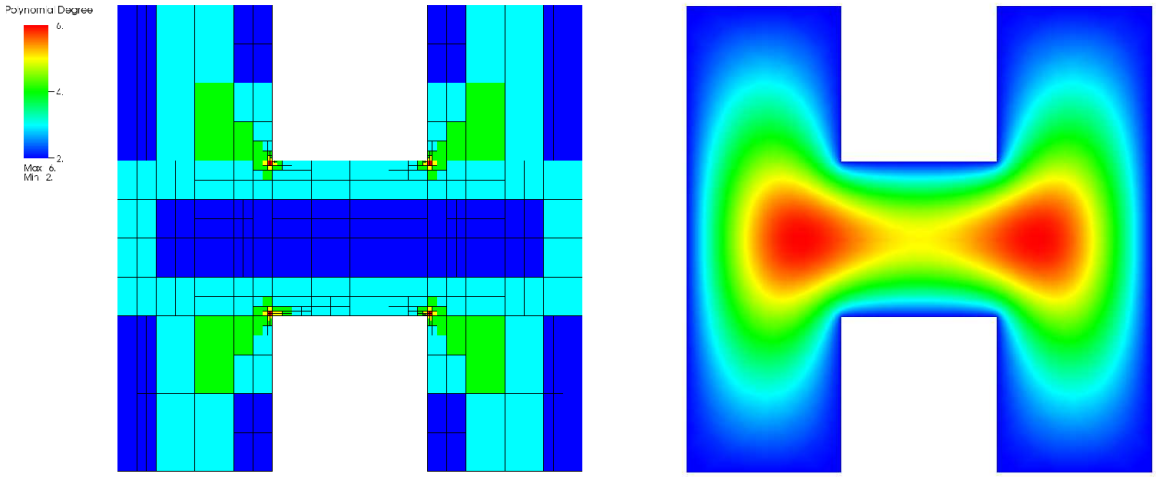

(a) (b)

Fig. 5 Example 2: (a) Mesh after 11 anisotropic adaptive refinement steps and (b) first eigenfunction.

4.3 Example 3

In our final example we consider problem (1.1) with $\Omega = (0,1)^2$ and discontinuous diffusion so that $\mathrm{A}_{ij} = 0$, $i \neq j$ and for $i = 1, 2$

$$\mathrm{A}_{ii} = \begin{cases} 1 & 0.45 < x < 0.55, \\ 100 & \text{otherwise.} \end{cases}$$

DOF	$\lvert\lambda_1 - \lambda_{1,hp}\rvert$	η_1^2	Effectivity
63	1.4764	56.00	37.93
90	1.5189	45.82	30.17
144	1.4188	28.23	19.90
180	2.783E-01	16.20	17.46
315	7.2706E-01	9.922	13.65
459	4.3041E-01	5.613	13.04
685	2.4699E-01	3.386	13.71
1129	1.0258E-01	1.051	10.25
2022	2.9340E-02	2.917E-01	9.94
3534	8.7951E-03	9.980E-02	11.35
6162	2.0569E-03	2.465E-02	11.98
9071	5.7294E-04	7.192E-03	12.55
12673	1.4432E-05	2.569E-03	17.80
16514	4.6869E-06	9.5572E-04	20.42

Table 2 Example 2: Anisotropic *hp*–strategy effectivities.

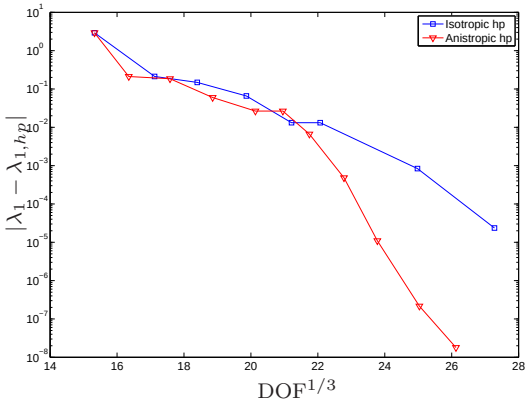

Fig. 6 Example 3: Comparison of isotropic *hp*– and anisotropic *hp*–strategy.

Again, the eigenvalues and eigenfunctions of this problem are unknown, but calculations on an extremely fine mesh reveal that the first eigenvalue has value 852.527814501 to the accuracy of our computations. Comparisons between anisotropic and isotropic *hp*–strategies are shown in Figure 6, again the anisotropic strategy is seen to be far superior than the isotropic one. Note that the initial mesh was chosen so that the discontinuities in A occurred only along elemental boundaries and not in their interior. Again, in Table 4.3 we show the effectivities as the mesh is refined. For this example the initial values of the effectivity index are quite huge probably due to the fact that the initial mesh is very coarse compared to the size of the inclusion. Also comparing with Example 1 and Example 2, the effectivity index seems to settle to a greater value. This can be explained in view of the fact that the hidden constant in (3.36) may depend on A.

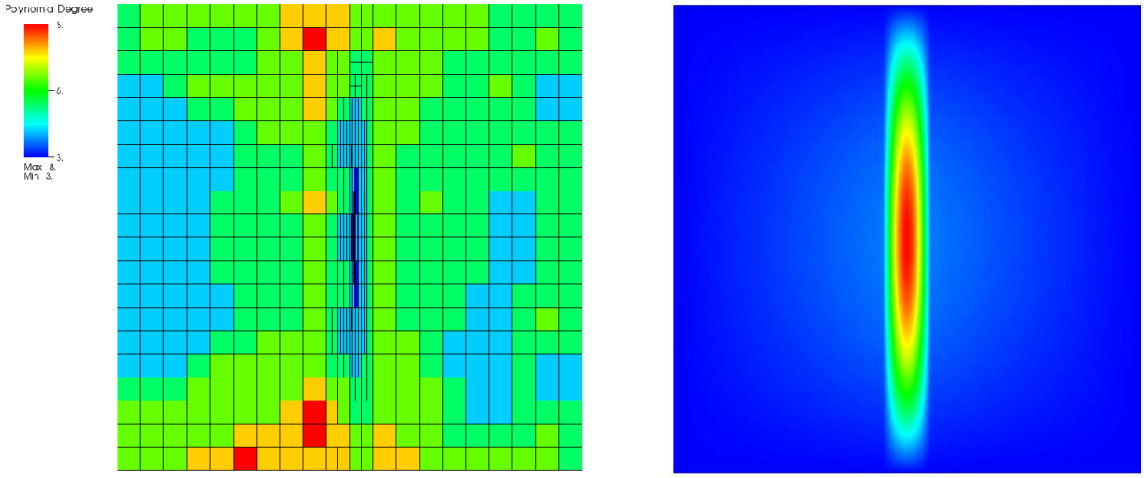

(a) (b)

Fig. 7 Example 3: (a) Mesh after 12 anisotropic adaptive refinement steps and (b) first eigenfunction.

DOF	$\lvert\lambda_1 - \lambda_{1,hp}\rvert$	η_1^2	Effectivity
3600	2.9216	9.079E+04	31074.38
4372	2.1164E-01	1.218E+03	5755.31
5436	1.8483E-01	3.700E+02	2001.98
6705	5.9894E-02	1.460E+02	2438.09
8163	2.6519E-02	54.73	2063.76
9203	2.6517E-02	23.31	878.95
10287	6.6503E-03	3.744E-01	56.30
11825	4.8241E-04	2.650E-02	54.94
13444	1.0998E-05	2.450E-03	222.82
15690	2.1629E-07	0.2.992E-05	138.33
17836	1.7958E-08	1.068E-06	59.45

Table 3 Example 3: Anisotropic *hp*–strategy effectivities.

References

1. D. Boffi, Finite element approximation of eigenvalue problems, *Acta. Numerica* 19:1-120,2010.
2. D.N. Arnold, F. Brezzi, B. Cockburn and D.L. Marini, Unified Analysis of Discontinuous Galerkin Methods for Elliptic Problems, *SIAM J. Numer. Anal.* 39(5):1749-1779, 2001.
3. S. Prudhomme, F. Pascal, J. T. Oden, and A. Romkes, Review of a priori error estimation for discontinuous Galerkin methods, *Technical report, TICAM Report* , 00-27, Texas Institute for Computational and Applied Mathematics, 2000.
4. J. Descloux, N. Nassif, and J. Rappaz , On spectral approximation. Part 1. The problem of convergence, *RAIRO - Analyse numerique*, 12(3):97-112, 1978.
5. J. Descloux, N. Nassif, and J. Rappaz , On spectral approximation. Part 2. Error estimates for the Galerkin method, *RAIRO - Analyse numerique*, 12(3):113-119, 1978.

6. P. Antonietti, Domain Decomposition, Spectral Correctness and Numerical Testing of Discontinuous Galerkin Methods, *PhD thesis*, 2006.
7. P. Antonietti, A. Buffa and I. Perugia, Discontinuous Galerkin approximation of the Laplace eigenproblem, *J. Comput. Appl. Math.* 204(2):317-333, 2007.
8. A. Ern, A. Stephansen and P. Zunino, A discontinuous Galerkin method with weighted averages for advection-diffusion equations with locally small and anisotropic diffusivity, *IMA J. Numer. Anal.* 20(2):235-256,2009.
9. L. Zhu, S. Giani, P. Houston and D. Schötzau, Energy norm a-posteriori error estimation for hp-adaptive discontinuous Galerkin methods for elliptic problems in three dimensions, *M3AS* 21(2):267-306, 20011.
10. E.J.C Hall and S. Giani, Discontinuous Galerkin Methods for Eigenvalue Problems on Anisotropic Meshes, Enumath 2011. To Appear.
11. P. Houston, E. Süli and T. Wihler, A-posteriori error analysis of *hp*-version discontinous Galerkin finite-element methods for second-order quasi-linear elliptic PDEs, *IMA J. Numer. Anal.* 28:245-273, 2008.
12. O.A. Karakashian and F. Pascal, A posteriori error estimation for a discontinuous Galerkin approximation of second order elliptic problems *SIAM J. Numer. Anal.* 41:2374–2399, 2003.
13. E. M. Garau, P. Morin and C. Zuppa, Convergence of adaptive finite element methods for eigenvalue problems, *Math. Models Methods Appl. Sci.* 19(5):721-747, 2009.
14. L. Zhu and D. Schötzau, A robust a-posteriori error estimate for *hp*-adaptive DG methods for convection-diffusion equations *IMA J. Numer. Anal.*
15. R. Verfürth, A Review of Posteriori Error Estimation and Adaptive Mesh Refinement Techniques *IWiley-Teubner* 1996.
16. P. Houston, D. Schötzau and T. Wihler, Energy norm a-posteriori error estimation of hp-adaptive discontinuous Galerkin methods for elliptic problems *Math. Models Methods Appl. Sci.* 17(1):33-62, 2007.
17. I. Perugia and D. Schötzau, An *hp*-analysis for the local discontinuous Gelrkin method for diffusion problems *J. Sci. Comput.* 17:561-571, 2002.
18. I. Perugia and D. Schötzau, The hp-Local Discontinuous Galerkin Method for Low-Frequency Time-Harmonic Maxwell Equations *Math. Comp.* 72(243):1179-1214, 2003.
19. J. T. Oden, I. Babŭska and C. E. Baumann, A discontinuous hp finite element method for diffusion problems, *TICAM Report 97-21, The University of Texas at Austin, 1997.*
20. J. T. Oden, I. Babŭska and C. E. Baumann, A discontinuous hp finite element method for diffusion problems, *J. Comput. Phys.* 146:491-519, 1998.
21. P. Houston, C. Schwab and E. Süli, Discontinuous hp-finite element methods for advection-diffusion problems, *Technical Report no. 00/15, Oxford University Computing Laboratory, 2000.*
22. M. Petzoldt, Regularity and error estimators for elliptic problems with discontinuous coefficients, Weierstraß Institut, 2001.
23. K.A. Cliffe, E. Hall and P. Houston, Adaptive Discontinuous Galerkin Methods for Eigenvalue Problems arising in Incompressible Fluid Flows, *SIAM J. Sci. Comput.* 31:4607–4632, 2010.
24. V. Heuveline and R. Rannacher, A Posteriori Error Control for Finite Element Approximations of Elliptic Eigenvalue Problems, *Adv. Comp. Math* 15:107–138, 2001.
25. J. Descloux, N. Nassif and J. Rappaz, On spectra approximation. II. Error estimates for the Galerkin methods, *RAIRO Anal. Numér* 12(2):113-119, 1978.
26. S. Giani and I. Graham, A convergent adaptive method for elliptic eigenvalue problems, SIAM J. Numer. Anal. 47:1067–1091, 2009.
27. R.G. Durán, C. Padra and R. Rodriguez, A posteriori error estimates for the finite element approximation of eigenvalue problems, *Math. Models Methods Appl. Sci.* 13:1219–1229, 2003.
28. T.F. Walsh and G.M. Reese and U.L. Hetmaniuk, Explicit a posteriori error estimates for eigenvalue analysis of heterogeneous elastic structures, *Comput. Methods Appl. Mech. Engrg.* 196:3614–3623, 2007.
29. R. B. Lehoucq, D. C. Sorensen, and C. Yang, ARPACK Users' Guide: Solution of Large-Scale Eigenvalue Problems with Implicitly Restarted Arnoldi Methods, SIAM, 1998.

30. P.R. Amestoy, I.S. Duff and J.-Y. L'Excellent, Multifrontal parallel distributed symmetric and unsymmetric solvers, *Comput. Methods in Appl. Mech. Eng.* 184: 501-520, 2000.
31. P. Houston and E. Süli, A note on the design of hp-adaptive finite element methods for elliptic partial differential equations *Computer Methods in Applied Mechanics and Engineering* 194: 229-243, 2005.
32. C. Schwab, *p*- and *hp*- Finite Element Methods: Theory and Applications to Solid and Fluid Mechanics *Oxford University Press* 1999.
33. I. Babuška and J. Osborn, Finite element Galerkin approximation of the eigenvalues and eigenfunctions of selfadjoint problems *Math. Comp.* 52:275-297, 1989.
34. E. H. Georgoulis, Discontinuous Galerkin Methods on Shape-Regular and Anisotropic Meshes PhD Thesis, 2003.
35. E. J. .C. Hall, Anistropic Adaptive Refinement for Discontinuous Galerkin Methods PhD Thesis, 2007.
36. P. Houston, C. Schwab and E. Süli, Stabilized Hp-Finite Element Methods for First-Order Hyperbolic Problems *SIAM J. Numer. Anal.* 37(5): 1618-1643, 2000.
37. S. Giani and E. Hall, An a Posteriori Error Estimator for hp-Adaptive Discontinuous Galerkin Methods for Elliptic Eigenvalue Problems *M3AS*, accepted.
38. S. Giani, D. Schötzau and L. Zhu, An a-posteriori error estimate for *hp*-adaptive DG methods for convection-diffusion problems on anisotropically refined meshes *Comput Math Appl*, submitted.
39. L. Zhu, Robust A Posteriori Error Estimation for Discontinuous Galerkin Methods for Convection Diffusion Problems PhD Thesis, 2010.
40. E. Burman and A. Ern, Continuous interior penalty *hp*-finite element methods for advection and advection-diffusion equations *Math. Comp.* 76(259):1119-1141, 2007.
41. I. Babuška and B.Q. Guo, The h-p Version of the Finite Element Method for Domains with Curved Boundaries *SIAM J. Numer. Anal.* 25(4):0036-1429, 1988.